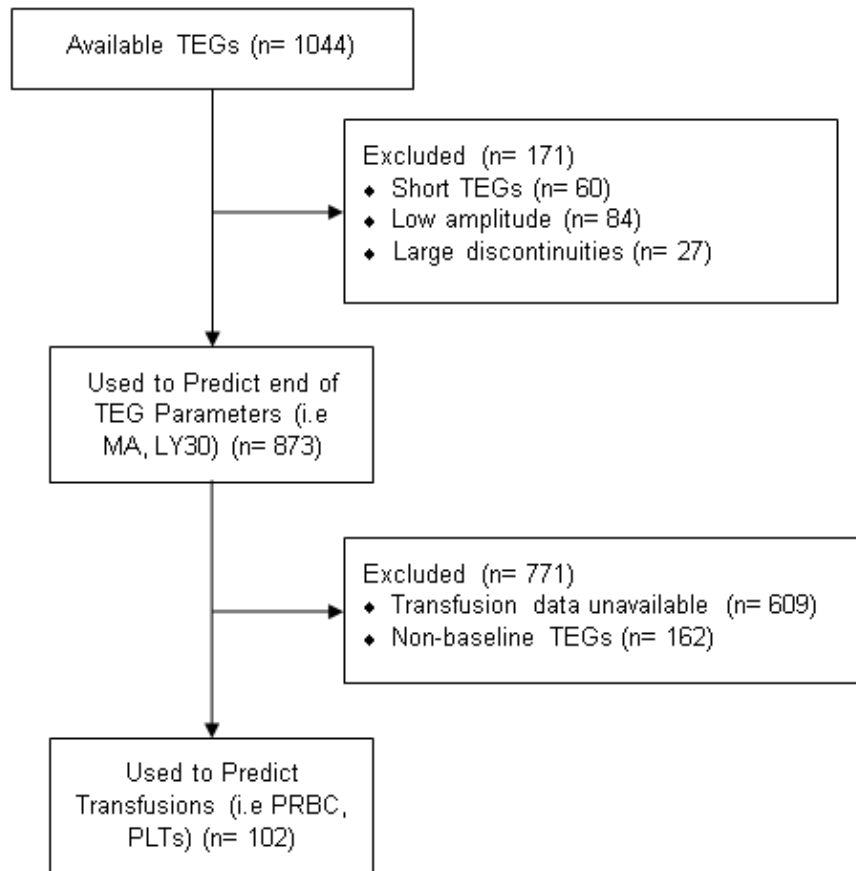


## Supplementary Digital Content

### *Division of TEGs into analyses performed*

The division of data into analyses is shown below in a CONSORT type diagram. The explicit procedure for removing discontinuous TEGs is in the next section (*Procedure for removing discontinuous TEGs*).



**Figure S1:** Diagram showing the filtering of TEG data for analysis.

## Procedure for removing discontinuous TEGs

A procedure was developed to determine and remove all TEGs with large jumps, and extremely low amplitudes (taking the total down from 1044 to 873 TEGs for full analysis). Two examples of TEGs removed from each category are shown. The process is as follows:

1. Remove all TEGs with less than 1000 seconds (~16 min) of data. This was to allow there to be enough data to work with for the algorithm, in addition to the fact that operators will stop a TEG early if there is something wrong (i.e. incorrect reagent added, someone hit the table during the TEG). Number removed for this reason: n=60.

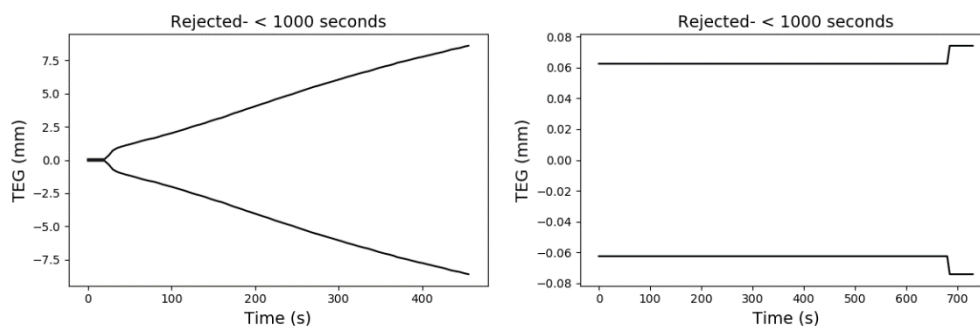


**Figure S2:** Examples of TEG data removed for containing < 1000 seconds of data.

2. Remove all TEGs with average amplitude of  $\leq 1$  mm for the top half of the TEG (or  $\leq 2$  mm for the full TEG). This removes all TEGs that never “kick-off”. Number removed for this reason: n=62.

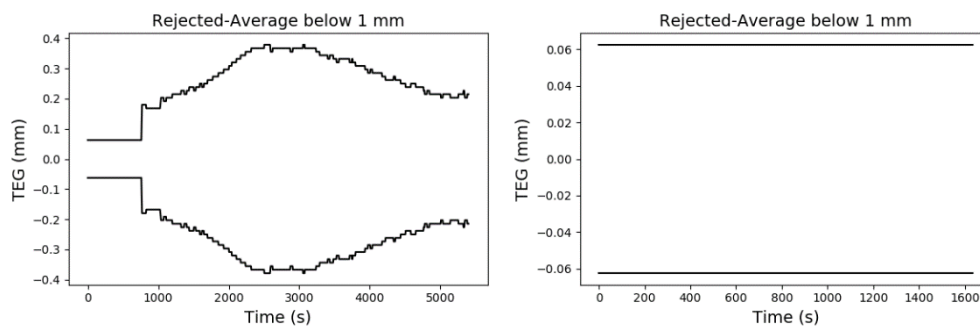


**Figure S3:** Examples of TEG data removed for averaging < 1 mm.

- Remove all TEGs with average amplitude of  $\leq 5$ mm for the top half of the TEG (or  $\leq 10$ mm for the full TEG) AND the MA  $< 7$ mm for the top half of the TEG (or  $\leq 14$ mm for the full TEG). This removes those with relatively low magnitudes that partially kick off, but never reach a reasonable MA. Number removed for this reason:  $n=22$ .

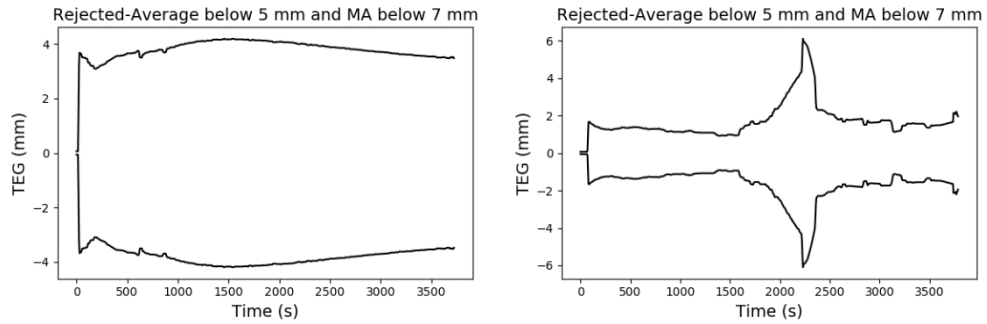


**Figure S4:** Examples of TEG data removed for averaging  $< 5$  mm and MA  $< 7$  mm.

- Remove all TEGs with large negative jumps between datapoints of a magnitude less than the maximum jump between any two data points (and negative jumps occur after 1000 seconds). Number removed for this reason:  $n=19$ .

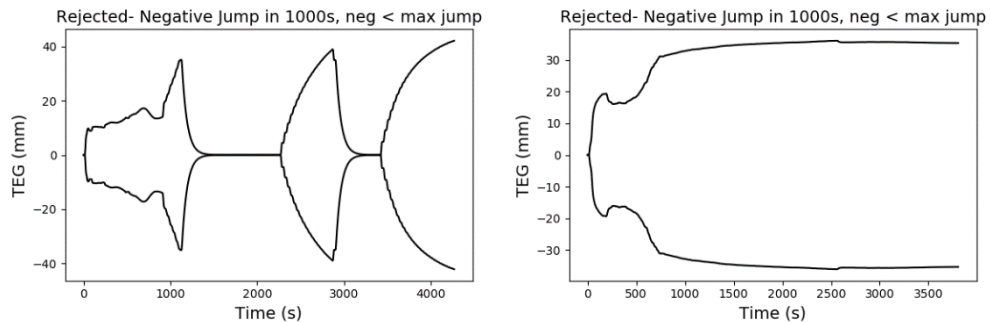


**Figure S5:** Examples of TEG data removed with negative jumps of magnitude less than the maximum jump in the data.

5. Remove all TEGs with a large jump in any direction  $>2.5$  mm for the top half of the TEG (or 5 mm for the full TEG) and contains negative jumps after 1000 seconds. These TEGs challenge the model in terms of fitting these discontinuities. Number removed for this reason:  $n=7$ .

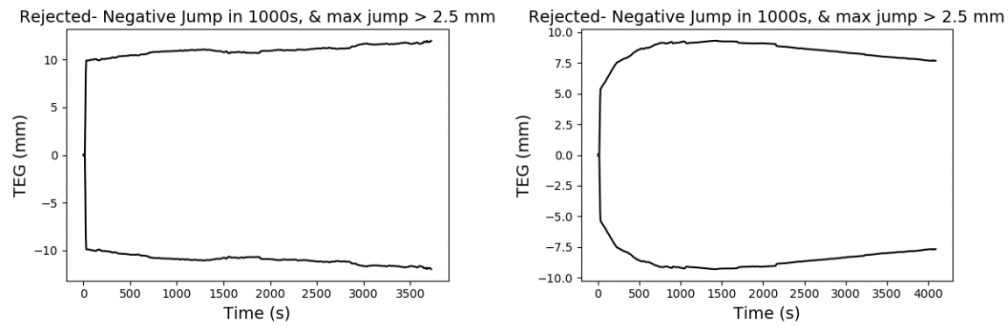


**Figure S6:** Examples of TEG data removed with large negative jumps and the maximum jump between two data points  $> 2.5$  mm.

### *Optimizing the number of nearest neighbors' effects*

It was necessary to analyze the effect of the KNN to pull from the over 160,000 simulations in the virtual library. This analysis was completed using the top 100 KNN and averaging the SSE for all RapidTEGs available. For five minutes of data, all SSE averages using the top 37 or less resulted in an average per point error of less than 0.5 mm. The maximum KNN to use was set at 20 and was chosen because of the increase in standard deviation of error for higher sample numbers (see below in Figure S1). However, it is of note that overall the differences in average resulting AUC's was <1% for the top 1, 10, 20, and 30 KNN. The top 10 KNN are shown in results.

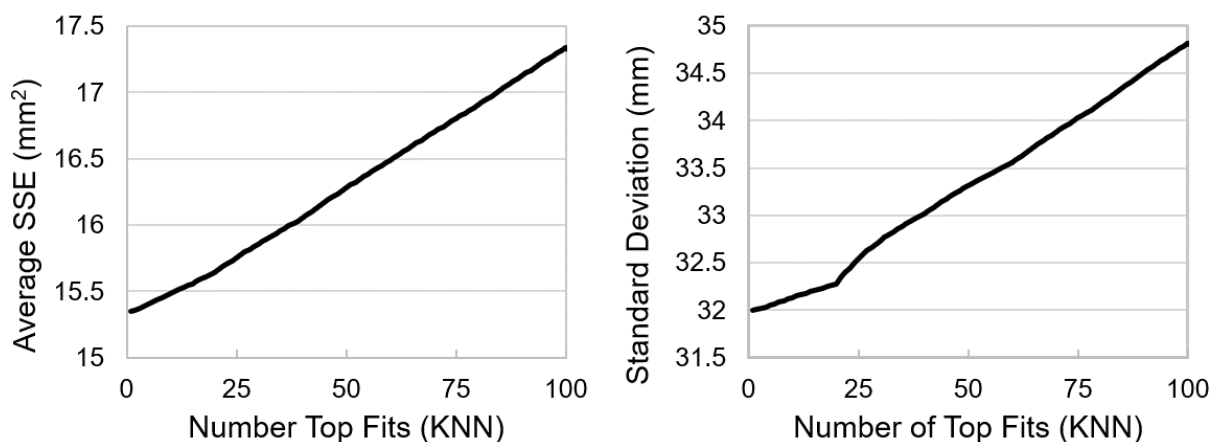


**Figure S7:** Plot showing the (left) average SSE and (right) standard deviation versus the number of top fits (KNN).

Additionally, comparing the variable changes in models built with different KNN was analyzed. The method to determine variables to include was stepwise LR. Stepwise LR parameters that improve the Akaike Information Criterion (AIC) for the top 1, 10 and 20 KNN are shown in Table S1. The result shows that adding additional neighbors results in more variables

being selected. As there are minimal differences between top 10 KNN and 20 KNN, the smaller of the two is used.

**Table S1:** Model parameters that are significant for predicting maximum amplitude of the TEG (MA), as calculated by stepwise logistic regression.

Time	Significant Parameters		
	1 KNN	10 KNN	20 KNN
3	P <sub>0</sub> , k <sub>1</sub> , k <sub>2</sub> , k <sub>3</sub> , SSE	P <sub>0</sub> , k <sub>1</sub> , k <sub>2</sub> , k <sub>3</sub> , SSE	P <sub>0</sub> , k <sub>1</sub> , k <sub>2</sub> , k <sub>3</sub> , SSE
4	P <sub>0</sub> , k <sub>1</sub> , k <sub>2</sub> , k <sub>3</sub> , SSE	P <sub>0</sub> , k <sub>1</sub> , k <sub>2</sub> , k <sub>3</sub> , SSE	P <sub>0</sub> , k <sub>1</sub> , k <sub>2</sub> , k <sub>3</sub> , SSE
5	P <sub>0</sub> , k <sub>1</sub> , k <sub>2</sub> , SSE	P <sub>0</sub> , k <sub>1</sub> , k <sub>2</sub> , k <sub>3</sub> , SSE	P <sub>0</sub> , k <sub>1</sub> , k <sub>2</sub> , k <sub>3</sub> , SSE
7.5	P <sub>0</sub> , k <sub>1</sub> , k <sub>2</sub>	P <sub>0</sub> , k <sub>1</sub> , k <sub>2</sub> , k <sub>3</sub> , SSE	P <sub>0</sub> , k <sub>1</sub> , k <sub>2</sub> , k <sub>3</sub> , SSE
10	P <sub>0</sub> , k <sub>1</sub> , k <sub>2</sub> , k <sub>3</sub>	P <sub>0</sub> , k <sub>1</sub> , k <sub>2</sub> , k <sub>3</sub>	P <sub>0</sub> , k <sub>1</sub> , k <sub>2</sub> , k <sub>3</sub>
15	P <sub>0</sub> , k <sub>1</sub> , k <sub>2</sub> , k <sub>3</sub>	P <sub>0</sub> , k <sub>1</sub> , k <sub>2</sub> , k <sub>3</sub> , SSE	P <sub>0</sub> , k <sub>1</sub> , k <sub>2</sub> , k <sub>3</sub> , SSE
20	P <sub>0</sub> , k <sub>1</sub> , k <sub>2</sub> , k <sub>3</sub>	P <sub>0</sub> , k <sub>1</sub> , k <sub>2</sub> , k <sub>3</sub> , SSE	P <sub>0</sub> , k <sub>1</sub> , k <sub>2</sub> , k <sub>3</sub> , SSE

### *Highlighted PRBC and PLT Predictions 24 hours after TEG start time*

Predictions were performed for 24 hours after TEG start time with similar performance to the 24 hours after admission. Figure S2A shows the predictions of PRBC transfusion after the TEG has started, and the accuracy approaches that of using the full TEG parameters with indistinguishable mean accuracy by 10 minutes. Clinically, this could provide useful estimates of imminent transfusion need. The case for this is strong for PLT transfusion shown in Figure S2B. Dynamic model parameters using the first 4 minutes of TEG data yield a predicted AUC outperforming that of the entire TEG tracing for predicting PLT transfusion in the first 24 hours (Figure S2B) with a median AUC of 0.75 using parameters established at four minutes versus median AUC of 0.64 for the full TEG parameters (p-value<0.0001).

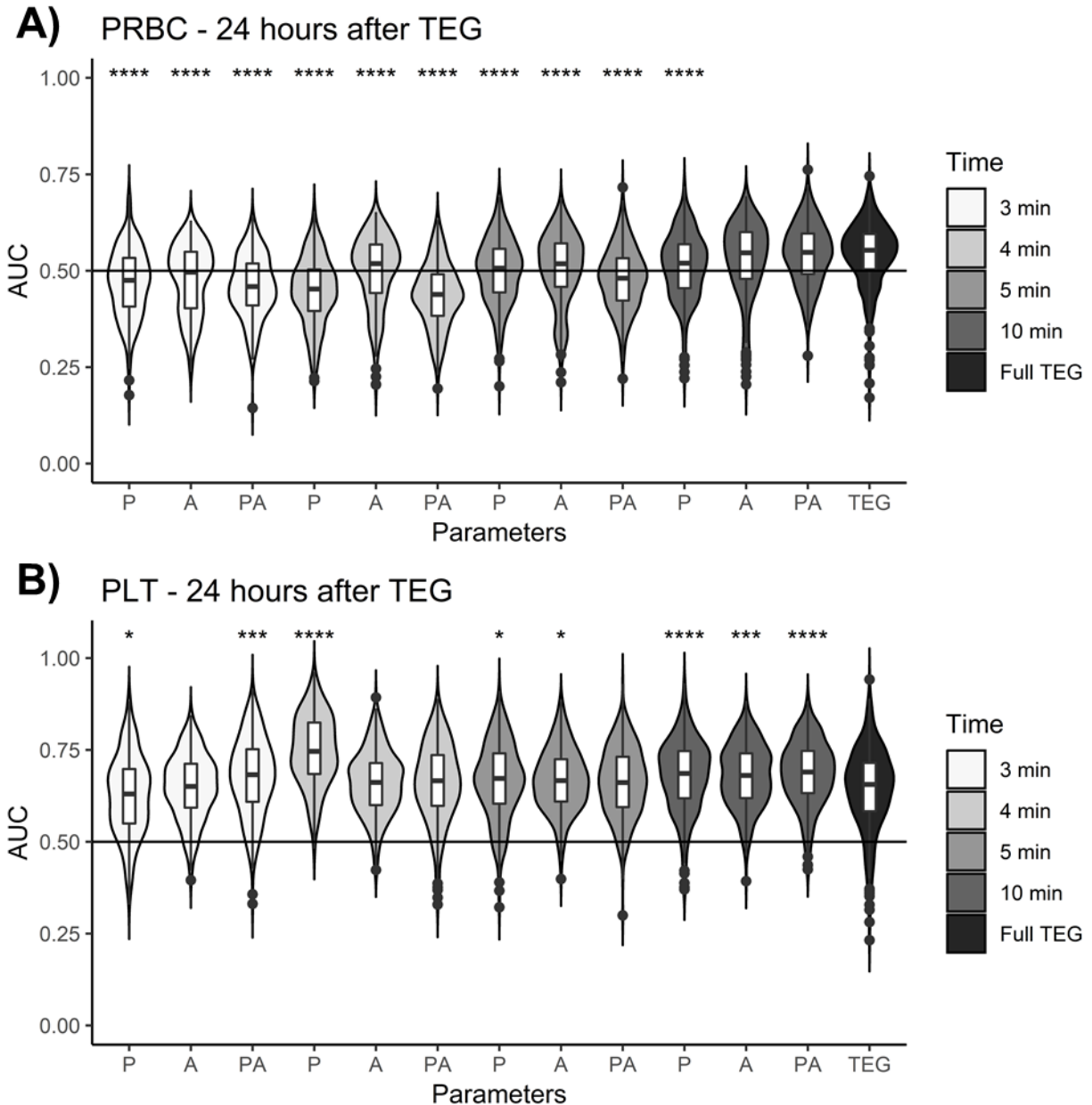


**Figure S8:** Accuracy (AUC of the ROC) of predictions of transfused blood products using the 10 KNN for the model parameters at 3, 4, 5, and 10 minutes, and using traditional TEG predictions (labeled: TEG), for: A) PRBC within the 24 hours after the TEG, and B) PLT within the 24 hours after the TEG. Lines are drawn at 50 percent accuracy to emphasize the points where estimates lose their clinical utility. P-value codes: \*\*: < 0.01, \*\*\*: < 0.001, \*\*\*\*: < 0.0001 comparing all distributions to the distribution generated using TEG parameters.



*Full transfusion predictions using model parameters (P), instantaneous amplitude (A), and a combined model (PA)*

While not all predictions result in useful or improved transfusion prediction, the full set of prediction AUCs are shown here in Figure S3. A subset is shown in the full text to highlight the relevant utility of the work. For PRBC transfusion, amplitude outperforms or equally performs compared to parameters from the model, or the combined model. However, the best performance is at longer time points or with full TEG parameters. For predicting PLT transfusion, initial performance using the 3, 4, and 5 minutes is particularly relevant. The model parameters at 4 minutes (P4) result in the prediction for an imminent (with 24 hours), and overall PLT transfusion with median AUCs of 0.66, and 0.57, respectively. Paired Wilcoxon tests were performed between each AUC distribution mean and the mean AUC distribution generated from using all TEG parameters (MA, TMA, alpha, k, R, TEGACT, LY30).

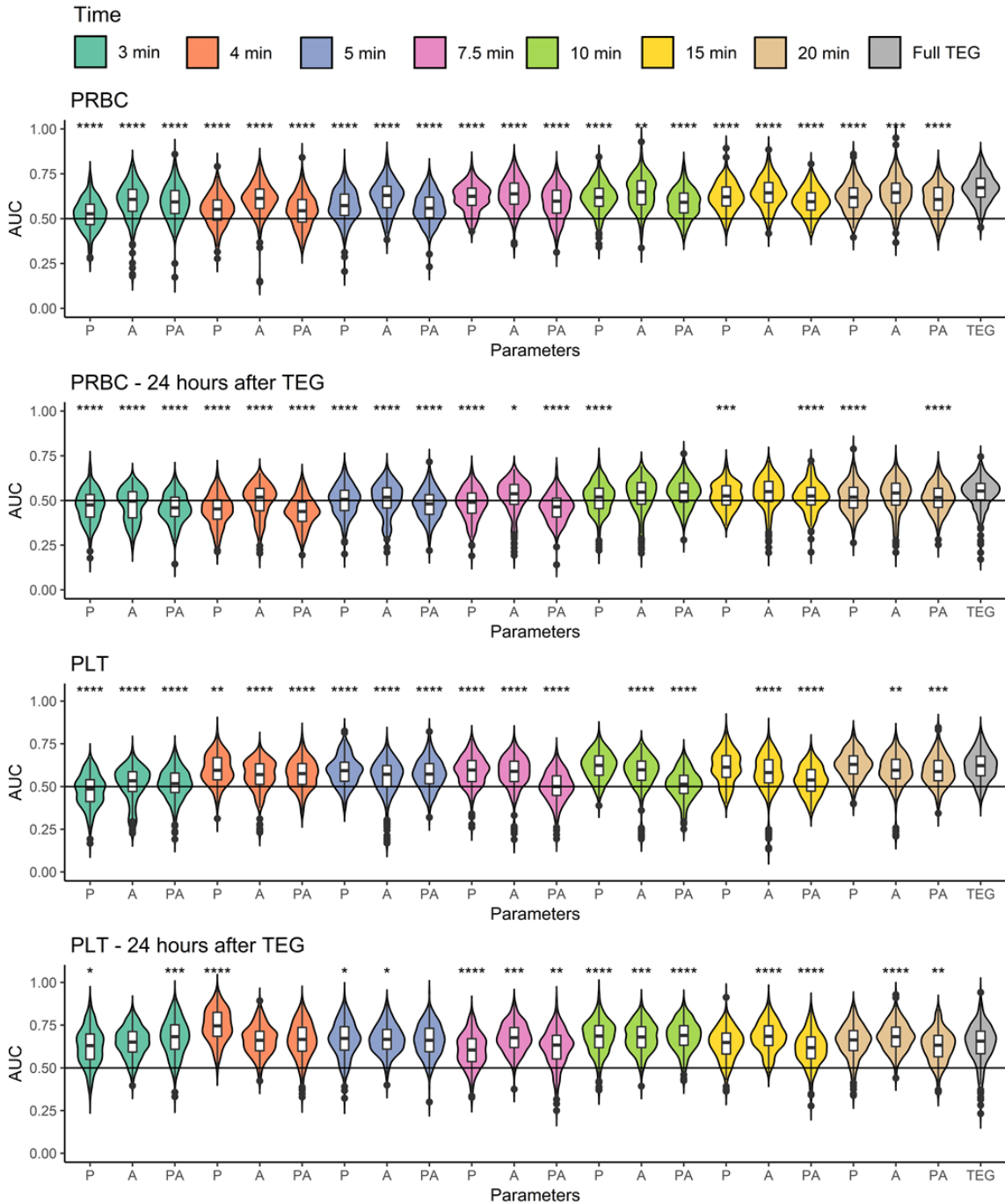


**Figure S9:** The full set of model parameters (P), instantaneous amplitude (A), and combined (PA) are shown at all time points (3, 4, 5, 7.5, 10, 15, 20 minutes). For predicting transfusion of PRBC, PRBC 24 hours after baseline TEG, PLT, and PLT 24 hours after baseline TEG, from top to bottom, respectively. P-value codes: \*\*: < 0.01, \*\*\*: < 0.001, \*\*\*\*: < 0.0001.

*Model Performance: Highest SSE fits to RapidTEG data*

To highlight the model's performance and more specifically the weaknesses, Figure S4 shows the top half the TEG along with the model fits to that data for the 4 highest SSE RapidTEGs. The SSE for Figure S4A is 21400 mm<sup>2</sup> and represents the worst fit RapidTEG in the set. This is primarily because the data shows two distinct rises, a structure that the model is incapable of capturing, therefore the optimal solution splits the difference. Figure S4B shows a RapidTEG with SSE of 8100 mm<sup>2</sup>. The model splits the middle of the data with the irregularities that occur around 2500 seconds. While generally, the model captures lysis well, Figure S4C and S4D show TEGs with 5500 and 4400 mm<sup>2</sup>, representing that there is a potential the model could capture high lysis patient TEGs better.

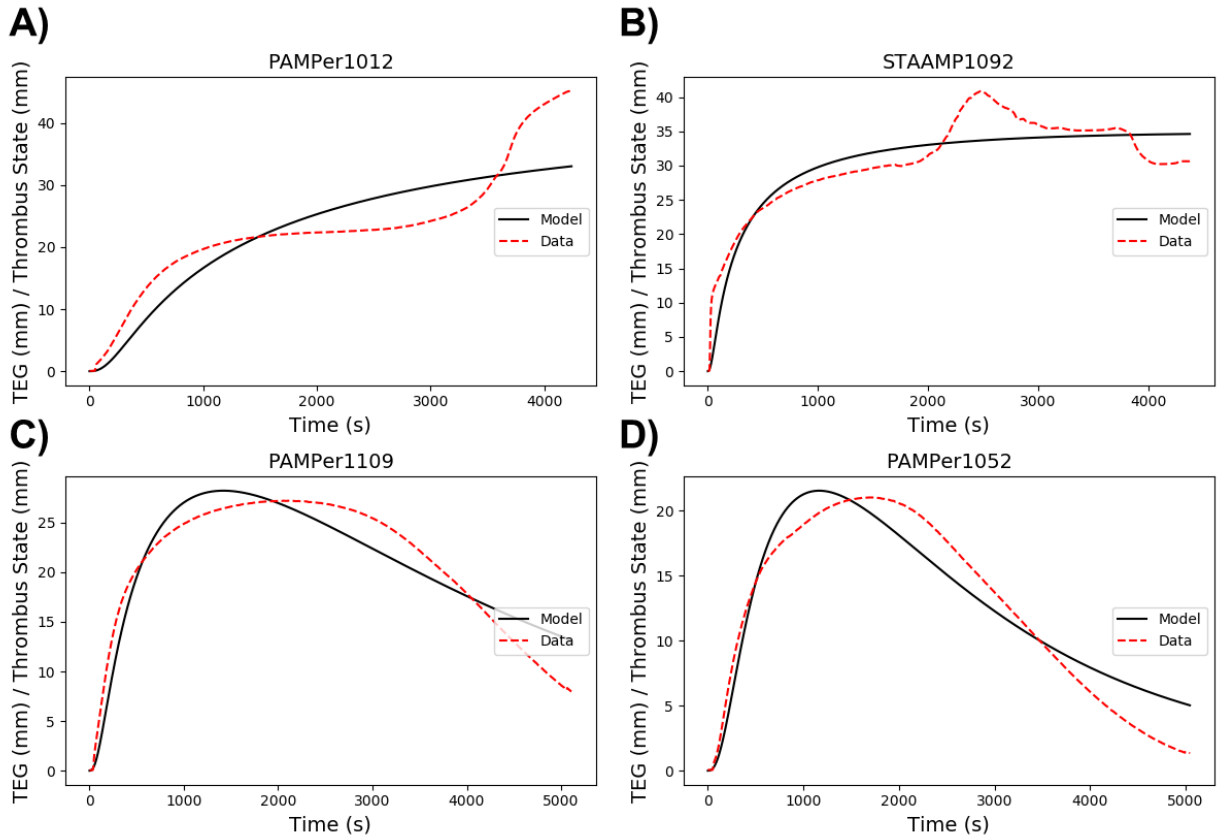


**Figure S10:** The worst 4 fit TEGs using the dynamic model optimization defined in the methods.

Showing A) the worst fit patient TEG, B) second worst fit patient TEG, C) third worst fit patient TEG, and D) fourth worst fit patient TEG, as measured by the sum of squared error (SSE).

*Predicting lysis at all time points*

Using models with model parameters (P), instantaneous amplitude (A), and a combination (PA), the lysis prediction accuracy metrics are shown in Figure S4.

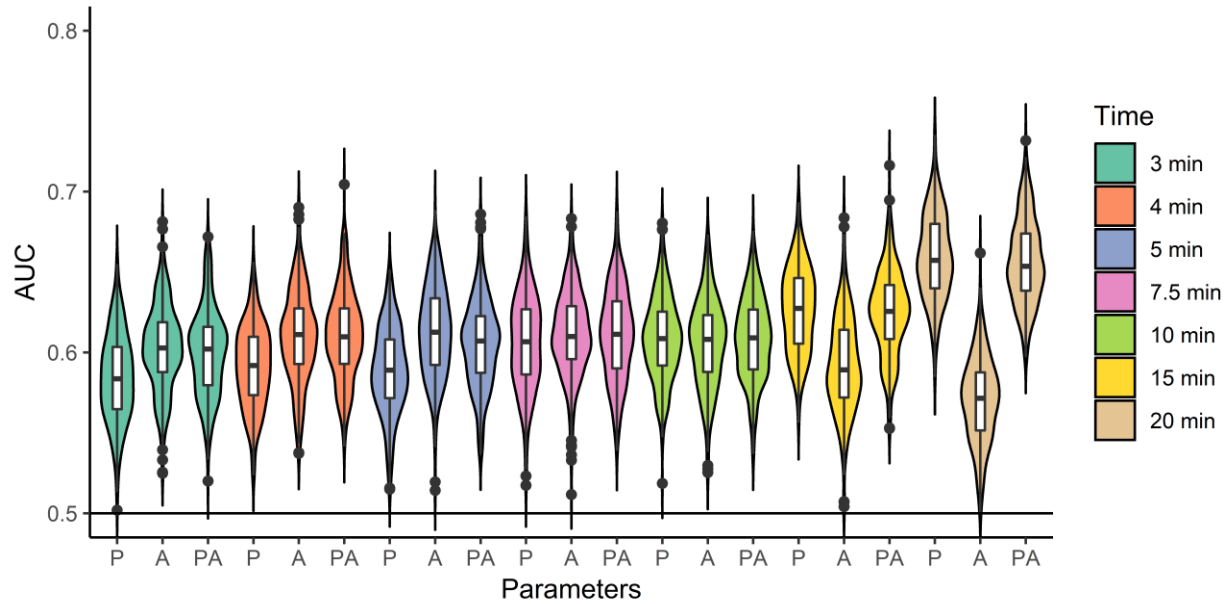


**Figure S11:** Plot showing the distribution of the AUCs predicting high lysis ( $LY_{30} \geq 3\%$ ) from using model parameters (P), instantaneous amplitude (A), and both (PA), at all time points (3, 4, 5, 7.5, 10, 15, 20 minutes).

## Predicting plasma transfusion at all time points

Using models with model parameters (P), instantaneous amplitude (A), and a combination (PA), the prediction accuracy metrics are shown in Figure S5 for predicting fresh frozen plasma (FFP) transfusion. Paired Wilcoxon tests were performed between each AUC distribution mean and the mean AUC distribution generated from using all TEG parameters (MA, TMA, alpha, k, R, TEGACT, LY30). This plot primarily shows plasma predictions significantly less than the TEG parameters.

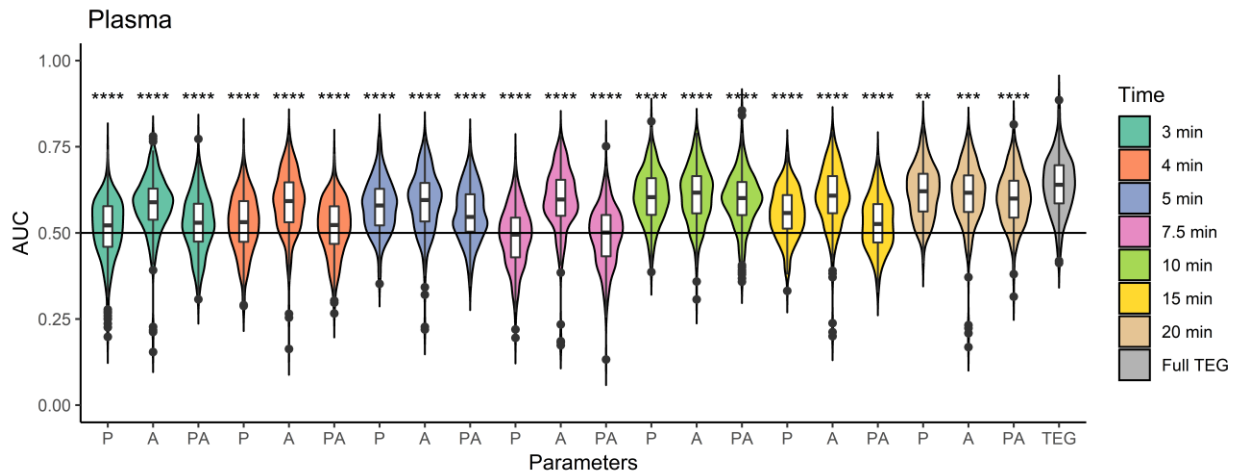


**Figure S12:** Plot showing the distribution of the AUCs predicting FFP transfusion from using model parameters (P), instantaneous amplitude (A), and both (PA), at all time points (3, 4, 5, 7.5, 10, 15, 20 minutes, along with the prediction using TEG parameters (MA, TMA, alpha, k, R, TEGACT, LY30). P-value codes: \*\*: < 0.01, \*\*\*: < 0.001, \*\*\*\*: < 0.0001. All distributions have means significantly less than the TEG parameter prediction of plasma transfusion need.

## Predicting MA: ROCs and Tuning Sensitivity and Specificity

For predicting MA using model parameters  $P(0)$ ,  $k_1$ ,  $k_2$ ,  $k_3$ , SSE and the instantaneous amplitude (at 3, 4, 5, 7.5, 10, 15, 20 minutes), the ROC curves from the test set for all the timespans with a randomized two-thirds train, one-third test split is shown in Figure S7A. Also, for the same time points the precision versus recall plot is shown in Figure S7B.

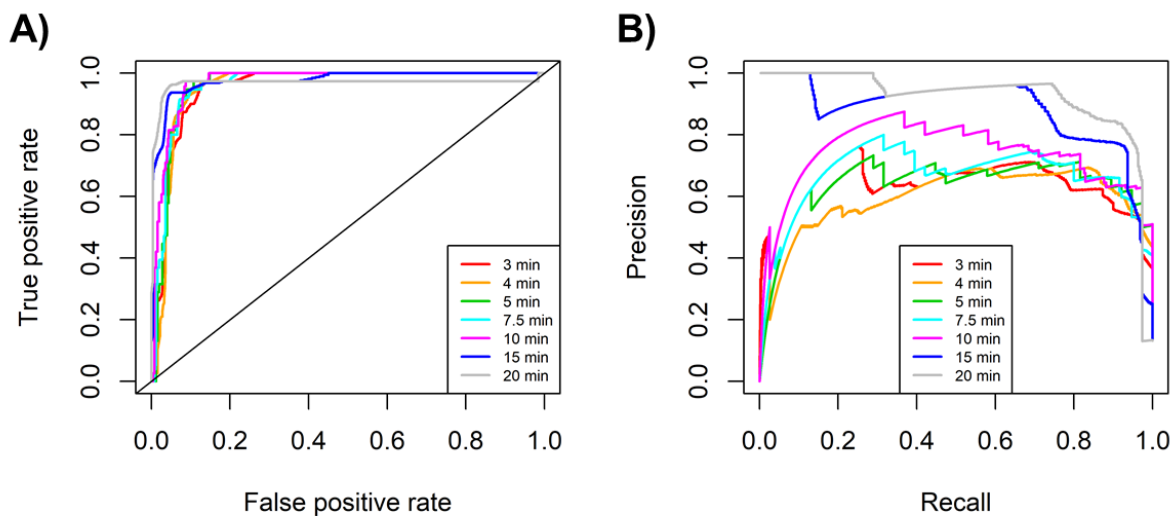


**Figure S13:** Plot of the **A)** Receiver Operating Characteristic (ROC) curves and the **B)** Precision vs. Recall curve from the LR using the following features: the model parameters ( $P(0)$ ,  $k_1$ ,  $k_2$ ,  $k_3$ ), the Sum of Squared Error (SSE) between the simulation and data up the time the test is performed (3, 4, 5, 7.5, 10, 15, 20 minutes), and instantaneous amplitude at 3, 4, 5, 7.5, 10, 15, 20 minutes. Thus, totaling the number of features used in the predictions as six.

Further analysis of the LR model looks at the LR predicted estimate of risk for each TEG and how the implementation of a threshold can be altered to affect the sensitivity and specificity from the resulting predictions. Depending on the application and desired outcome, a tuned threshold can be established to minimize false positive or false negatives, or to strike a balance between the two. In this way, varying threshold can change specificity and sensitivity for MA

predictions which is shown in Figure S5. At a threshold of 0.2, the specificity has been raised above 70 percent and the sensitivity remains above 90 percent, striking a desired balance between the false positive and negatives.

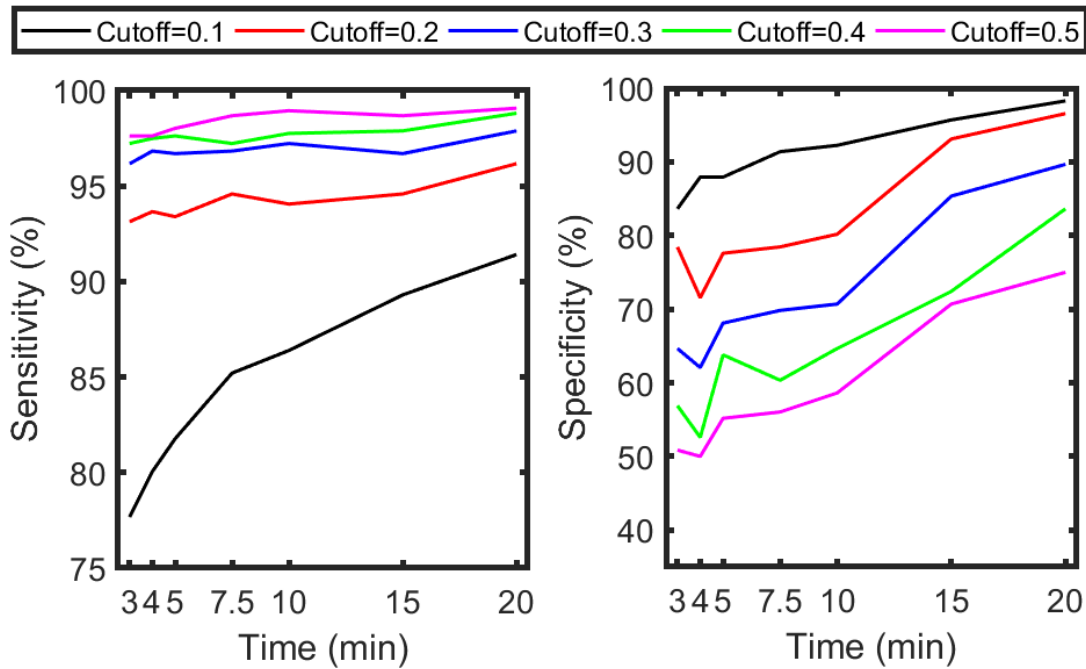


**Figure S14:** Plot of the sensitivity (left) and specificity (right) versus the specified time window (3, 4, 5, 7.5, 10, 15 or 20 minutes) used in the algorithm. In the legend, the different cutoff values used to distinguish patients with MA problem or not from their predicted risk from the LR are shown by the different colors.



## Parameter differences versus MA

Changes in parameters motivate the choice of LR as a model structure to attempt to classify MA problems. Plots of parameters versus MA for the RapidTEGs is shown in Figure S6 using only 3 minutes of data and the nearest neighbor.

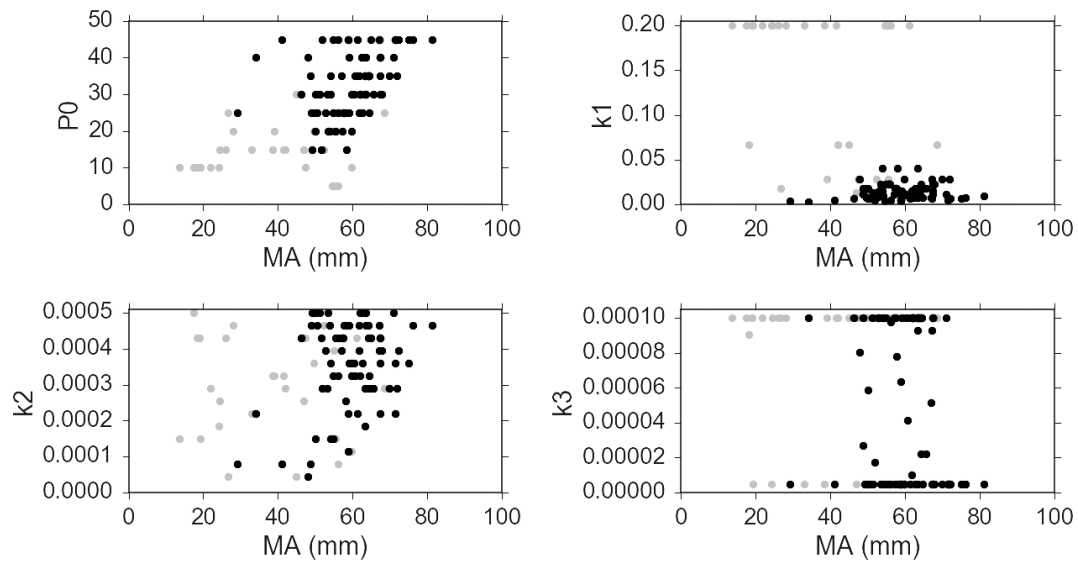


**Figure S15:** Plot showing the dynamic parameters versus the actual MA from 3 minutes of data, with the colors showing the predictions. Points in black were predicted above the clinical threshold and points in grey were predicted below the clinical threshold. The four plots show the four different parameters (P0 – top left, k1 – top right, k2 – bottom left, and k3 – bottom right).